Numerical Study of Resistive Magnetohydrodynamic Mode Structures in Typical Plasmas of the Large Helical Device

Yutaka MATSUMOTO[1), Kiyomasa WATANABE[2) and Luis GARCIA[3)

[1)*Graduate School of Engineering, Hokkaido University, Sapporo 060-8628, Japan*
[2)*National Institute for Fusion Science, Toki 509-5292, Japan*
[3)*Universidad Carlos III, Madrid, Spain*

(Received 10 January 2006 / Accepted 24 January 2006)

We study the resistive instabilities typically observed in the Large Helical Device (LHD) in order to systematically investigate the effects of the resistive magnetohydrodynamics (MHD) instabilities on the plasma confinement. The resistive instabilities with the low toroidal mode number are investigated by using the three-dimensional linear resistive MHD code FAR3D. It is confirmed that both the growth rate and the mode width obey the theoretical formula of the gravitational interchange mode independent of the toroidal mode number. The range of the magnetic Reynolds number, in which the growth rate and/or the mode width obey the theoretical formula, is clarified. It is found that the growth rate is proportional to the mode width when beta is constant.

Keywords: resistive MHD, LHD, FAR3D

DOI: 10.1585/pfr.1.001

1 Introduction

It is important to understand the magnetohydrodynamic (MHD) equilibrium and stability properties for the realization of the nuclear fusion reactor. In a helical device, such as the Large Helical Device (LHD)[1] in Japan, the complex three-dimensional (3D) MHD study is needed for the successful operation. The MHD instability modes typically observed in the LHD experiments are summarized as follows. Some modes, of which the dependence property on the magnetic Reynolds number is similar to the resistive gravitational interchange mode[2], are obtained in the peripheral region of the high beta plasma with the strong magnetic shear. Others are frequently monitored in the core region of the high aspect ratio plasma with the relatively weak magnetic shear.

It is the purpose of this study to systematically investigate the effects of the resistive MHD instability on the plasma confinement in the LHD. Consequently, the typical MHD instability modes are numerically analyzed by using the 3D resistive MHD code FAR3D[3]. We especially focus on the mode width, i.e., the resistive layer thickness and systematically investigate the relationships between mode width (W), beta ($\langle\beta\rangle$), growth rate (γ) and magnetic Reynolds number (S).

In this paper, the resistive MHD instability modes in the high beta plasma with the strong magnetic shear are described. The outline of the FAR3D code and the numerical conditions are given in Section 2. The results of the calculations are summarized in Section 3. Section 4 is devoted to a brief summary.

author's e-mail: shopon@qe.eng.hokudai.ac.jp

2 Numerical Model

As mentioned in the preceding section, the FAR3D code is a 3D resistive MHD code[3]. In this code, a set of resistive MHD equations is time-advanced in the Boozer coordinates[4]. And the perturbed quantities are expanded in Fourier series in the generalized poloidal and toroidal angles by using the poloidal mode number (n) and the toroidal mode number (m). FAR3D appears in different forms depending on the approximation and the treatment for the MHD equations. We adopt one of the some versions of FAR3D, in which the reduced equations[3]:

$$\frac{\partial\psi}{\partial t} = \nabla_{\mathrm{p}}\Phi + \eta B_{\zeta}^{\mathrm{eq}} J_{\zeta}, \tag{1}$$

$$\begin{aligned}\frac{\partial U}{\partial t} &= -\boldsymbol{v}\cdot\nabla U \\ &+ S^{2}\left\{\frac{\beta_0}{2\epsilon^2}\left(\frac{1}{\rho}\frac{\partial\sqrt{g}}{\partial\theta}\frac{\partial p}{\partial\rho} - \frac{\partial\sqrt{g}}{\partial\rho}\frac{1}{\rho}\frac{\partial p}{\partial\theta}\right)\right. \\ &+ \left.\nabla_{\mathrm{p}} J^{\zeta} - \frac{1}{\rho}\frac{\partial}{\partial\rho}\left(\rho J_{\mathrm{eq}}^{\zeta}\right)\frac{1}{\rho}\frac{\partial\psi}{\partial\theta}\frac{1}{\rho}\frac{\partial J_{\mathrm{eq}}^{\zeta}}{\partial\theta}\frac{\partial\psi}{\partial\rho}\right\},\end{aligned} \tag{2}$$

and

$$\frac{\partial p}{\partial t} = -\boldsymbol{v}\cdot\nabla p + \frac{\mathrm{d}p_{\mathrm{eq}}}{\mathrm{d}\rho}\frac{\partial\Phi}{\partial\theta}, \tag{3}$$

are linearly calculated, where the velocity and the magnetic field are described as $\boldsymbol{v} = \sqrt{g}\nabla\zeta\times\nabla\Phi$ and $\boldsymbol{B} = R_0\nabla\zeta\times\nabla\Psi$, respectively.

The used MHD equilibria, i.e., the high beta plasma with the strong magnetic shear, is generated by using the 3D equilibrium code VMEC[5]. The equilibrium is described by using 1,000 radial grid points, and 20 helical

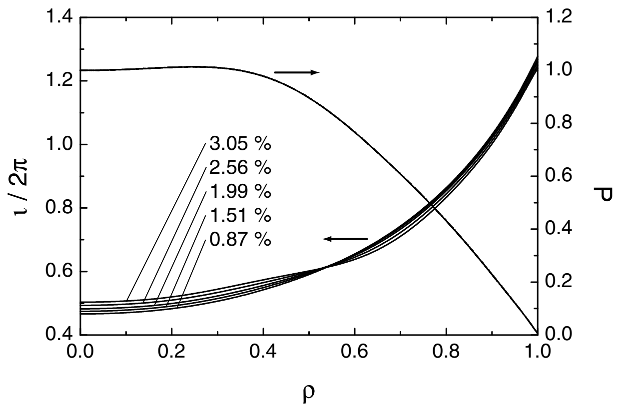

Fig. 1 Radial profiles of $\iota/2\pi$ and P in the equilibrium using in this study.

($n \neq 0$) and 3 toroidal ($n = 0$) Fourier modes. Figure 1 shows the rotational transform ($\iota/2\pi$) and the pressure (P) of the used equilibrium, in which the volume-averaged beta ($\langle\beta\rangle$) are 0.87, 1.51, 1.99 2.56, and 3.05 %, respectively.

In this paper, the resistive instabilities with the low toroidal mode numbers ($n = 1, 2, 3$) are described. It is seen from Fig. 1 that there are the rational surfaces of $m/n = 1/1, 2/1, 2/2, 3/2, 4/2, 3/3, 4/3, 5/3, 6/3$.

As mentioned in Section 1, we pay attention to the mode width, i.e., the resistive layer thickness. The mode width (W) is defined as the region that the growing speed of the instability to the radial direction (V_ρ) is larger than 70 % of the peak value. It is noted that $\partial\xi/\partial t = V_\rho$, where ξ is the perturbation to the radial direction. A example of the radial profiles of V_ρ, i.e., the mode structure, is shown in Fig.2.

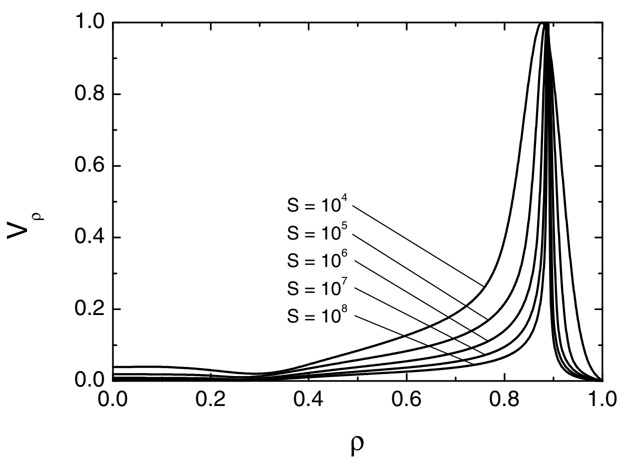

Fig. 2 Radial profiles of V_ρ of $m/n = 1/1$ modes in the case of $\langle\beta\rangle = 1.99$ %.

3 Results

3.1 $n = 1$ mode

In the cases of $\langle\beta\rangle \le 1.51$ %, both $m/n = 1/1$ and $2/1$ modes are unstable and their peak values of V_ρs are almost the same. When the calculation without the $m/n = 2/1$ mode is done to determine the primary unstable mode, γ remains the same as the results of the calculations including the $m/n = 2/1$ mode. Both $m/n = 1/1$ and $2/1$ modes also appear in the cases of $\langle\beta\rangle \ge 1.99$ %. In these cases, the peak value of V_ρ of $m/n = 1/1$ mode is larger than that of $m/n = 2/1$ mode and γ remains the same as the results of the calculation without $m/n = 2/1$ mode. Therefore, the $m/n = 1/1$ mode is the primary unstable mode. There exist the rational surfaces of $m/n = 1/1$ around $\rho \simeq 0.89$.

The relationships between S and γ are shown in Fig. 3, and the relationships between S and W are shown in Fig. 4. It can be seen from Figs. 3 and 4 that both γ and W are proportional to $S^{-1/3}$. This dependency is similar to the resis-

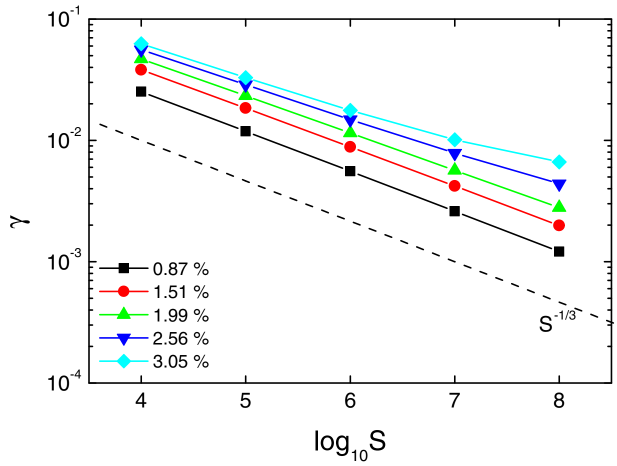

Fig. 3 Relationships between S and γ in the case of $m/n = 1/1$ mode.

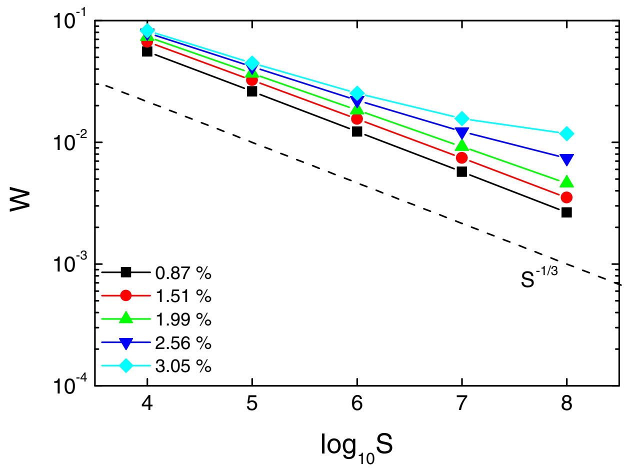

Fig. 4 Relationships between S and W in the case of $m/n = 1/1$ mode.

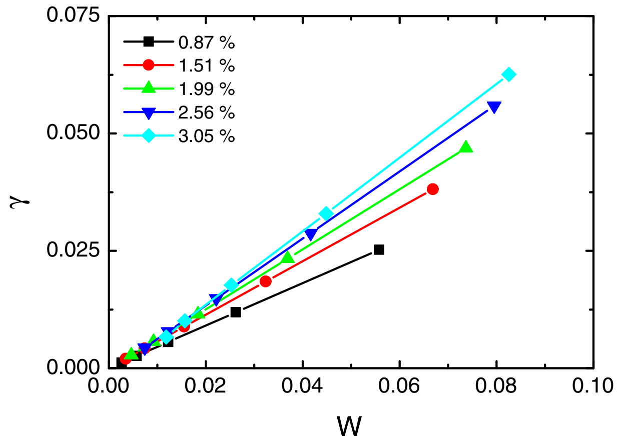

Fig. 5 Relationships between W and γ in the case of $m/n = 1/1$ mode.

tive gravitational interchange mode[2]. Such dependency of γ and W on S, however, becomes small when $\langle\beta\rangle = 3.05$ % and $\log_{10} S > 6$.

Figure 5 shows the relationships between W and γ. In each $\langle\beta\rangle$ cases, γ is proportional to W. The slopes become steep with $\langle\beta\rangle$ increasing.

3.2 $n = 2$ mode

In the case of $n = 2$, only the $m/n = 3/2$ mode is observed as the unstable mode. The rational surfaces of $m/n = 3/2$ exist around $\rho \simeq 0.63$.

The relationships between S and γ are shown in Fig. 6, and the relationships between S and W are shown in Fig. 7. Both γ and W are proportional to $S^{-1/3}$ in the case of $\langle\beta\rangle = 0.87$ %. When $\langle\beta\rangle \geq 1.51$ % and $\log_{10} S > 5$, however, γ and W are almost independent of S. Both γ and W of the $m/n = 3/2$ mode hardly increase with $\langle\beta\rangle$ in the cases of $\langle\beta\rangle \geq 1.99$ % γ of the $m/n = 3/2$ mode as well as γ of the $m/n = 1/1$ mode is proportional to W. The slopes also become steep with the increase of $\langle\beta\rangle$ (Fig. 8).

Compared these results of the $m/n = 3/2$ mode with those of the $m/n = 1/1$ mode, γ of the $m/n = 3/2$ mode is larger than that of the $m/n = 1/1$ mode. On the other hand, W of the $m/n = 3/2$ mode is slightly smaller than that in the $m/n = 1/1$ mode. The range of S, in which γ and $W \propto S^{-1/3}$, in $n = 2$ case is narrower than that in $n = 1$ case. In the cases of $\langle\beta\rangle \geq 2.56$ %, the dependency of γ and W on $\langle\beta\rangle$ in $n = 2$ case is smaller than that in $n = 1$.

3.3 $n = 3$ mode

In the case of $\langle\beta\rangle = 0.87$ %, only the $m/n = 5/3$ mode is unstable. The $m/n = 4/3$ unstable mode, however, appears in the calculations without the $m/n = 5/3$ mode. In this case, γ is larger than that in the calculation including the $m/n = 5/3$ mode. Although both $m/n = 4/3$ and $m/n = 5/3$ modes are unstable in the $\langle\beta\rangle = 1.51$ %

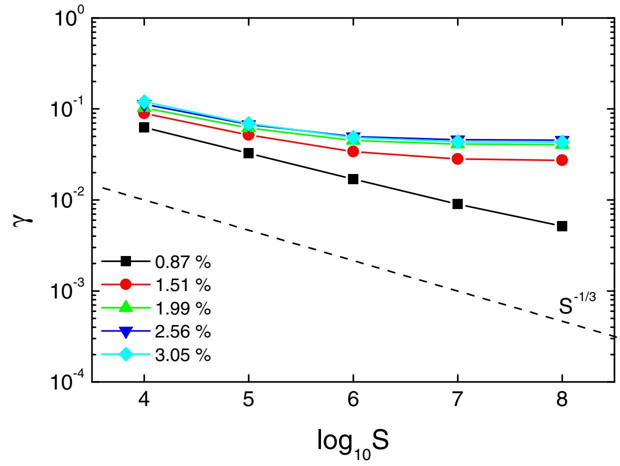

Fig. 6 Relationships between S and γ in the case of $m/n = 3/2$ mode.

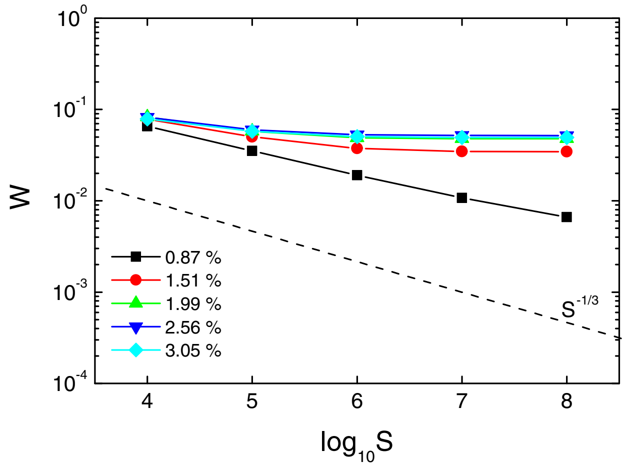

Fig. 7 Relationships between S and W in the case of $m/n = 3/2$ mode.

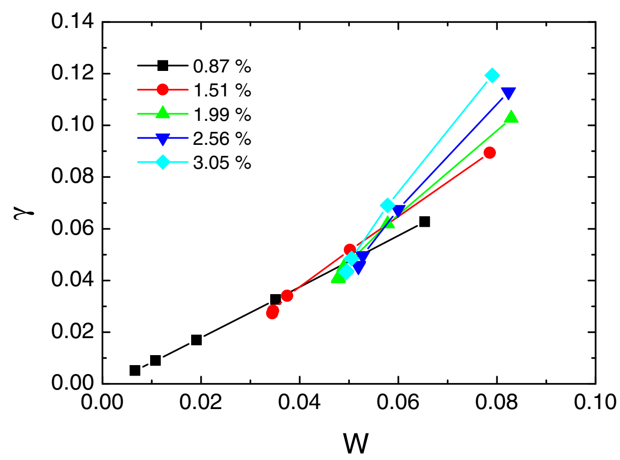

Fig. 8 Relationships between W and γ in the case of $m/n = 3/2$ mode.

case, V_ρ of the $m/n = 5/3$ mode is larger than that of the $m/n = 4/3$ mode. In the calculations without $m/n = 5/3$ mode, however, the $m/n = 4/3$ mode becomes unstable and its γ is larger than that in the calculation including the $m/n = 5/3$ mode. When $\langle\beta\rangle \geq 1.99$ %, both $m/n = 4/3$ and $m/n = 5/3$ modes are unstable. However, V_ρ of the $m/n = 4/3$ mode is larger than that of the $m/n = 5/3$ mode. These results indicate that $m/n = 4/3$ mode is the primary unstable mode. There are the rational surfaces of $m/n = 4/3$ around $\rho \simeq 0.72$.

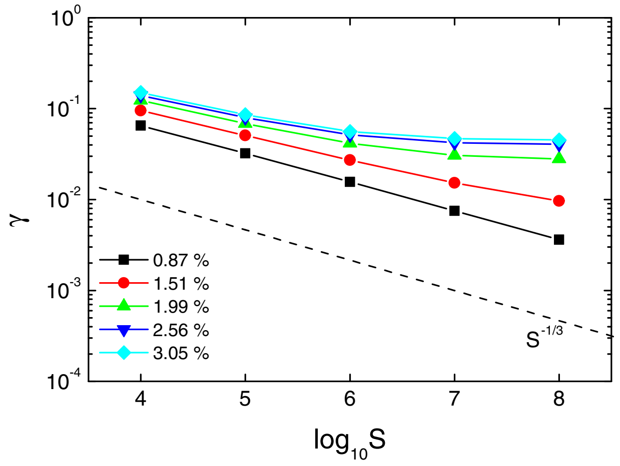

Fig. 9 Relationships between S and γ in the case of $m/n = 4/3$ mode.

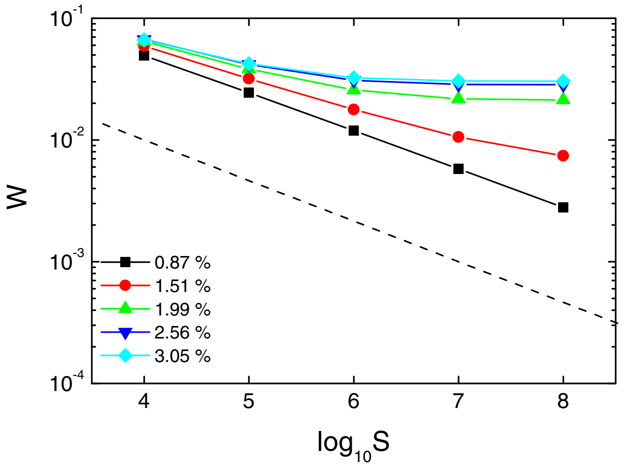

Fig. 10 Relationships between S and W in the case of $m/n = 4/3$ mode.

The relationships between S and γ are shown in Fig. 9, and the relationships between S and W are shown in Fig. 10. γ is proportional to $S^{-1/3}$ when $\langle\beta\rangle \leq 1.51$ %. On the other hand, W is proportional to $S^{-1/3}$ only if $\langle\beta\rangle = 0.87$ %. In high beta and $\log_{10} S > 6$ cases, the dependency of γ and W on S become small. Such changes of the dependency of W occur in lower beta cases than those of γ. The dependencies of γ and W of the $m/n = 4/3$ mode on $\langle\beta\rangle$ is as small as that of the $m/n = 3/2$ mode in the case of $\langle\beta\rangle \geq 2.56$ %. As shown in Fig. 11, γ of the $m/n = 4/3$ mode is also proportional to W and the slopes become steep with the increase of $\langle\beta\rangle$.

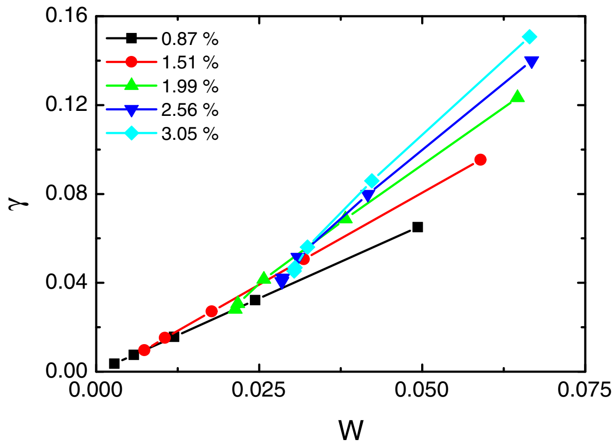

Fig. 11 Relationships between W and γ in the case of $m/n = 4/3$ mode.

Compared these results of $n = 1$, $n = 2$ and $n = 3$ modes, γ of $n = 3$ mode is the largest in three n cases. On the contrary, W of $n = 3$ mode is the smallest. The range of S, in which γ and $W \propto S^{-1/3}$, in $n = 3$ case is narrower than that in $n = 2$ case.

4 Summary

In this paper, the low n resistive instability modes in the typical LHD high beta plasma with the strong magnetic shear are analyzed by using the FAR3D code.

It is found that the primary unstable modes are $m/n = 1/1$, $3/2$, $4/3$. The rational surfaces of these modes exist in the plasma periphery ($\rho > 0.6$). It is confirmed that both γ and W obey the theoretical formula of the gravitational interchange mode($\propto S^{-1/3}$) independent of n. Their dependencies on S become small when $\langle\beta\rangle$ and/or S are high. The range of S, in which γ and/or W are proportional to $S^{-1/3}$, becomes narrow as n decreasing. When $\langle\beta\rangle = \text{const.}$, γ is proportional to W. The slope becomes steep with $\langle\beta\rangle$ increasing.

In near future, the resistive instabilities of $n > 4$ will be studied. In addition, the resistive instabilities in the different equilibrium of the LHD will also be investigated.

This work was supported by the collaborative research program of NIFS (NIFS06KLHH302).

[1] A. Iiyoshi *et al.*, Nucl. Fusion **39**, 1245 (1999).

[2] H. P. Furth, J. Killeen, M. N. Rosenbluth, Phys. Fluids **6**, 459 (1963) .

[3] L. Garcia, *Proc. 25th EPS Conf. on Controlled Fusion and Plasma Physics* (Prague, 1998), VOL. 22A, PartII, p. 1757.

[4] A. H. Boozer, Phys. Fluids **23**, 904 (1980).

[5] S. P. Hirshman, Phys. Fluids **26**, 3553 (1983).